

## Laser splitting of bilayer structures made of silicon wafers and glass substrates

Y.V. NIKITJUK<sup>1</sup>, A.N. SERDYUKOV<sup>1</sup>, I.Y. AUSHEV<sup>2</sup>

The paper presents the results of a finite-element simulation of the laser splitting process of bilayer structures of monocrystalline silicon and glass when the workpiece is exposed to laser beams with wavelengths equal to 0,808  $\mu\text{m}$  and 10.6  $\mu\text{m}$  and a refrigerant. The calculation of thermoelastic fields created in a bilayer wafer as a result of laser heating was performed for three cuts of silicon crystals, i.e. (100), (110), (111). The outcomes of this research can be used to optimize the process of laser separation of bilayer structures made of monocrystalline silicon and glass.

**Keywords:** laser splitting, silicon wafer, finite-element method.

В работе представлены результаты конечно-элементного моделирования процесса лазерного раскалывания двухслойных структур из монокристаллического кремния и стекла при воздействии на обрабатываемое изделие лазерных пучков с длинами волн равными 0,808 мкм и 10,6 мкм и хладагента. Расчет термоупругих полей, формируемых в двухслойной пластине в результате лазерного нагрева, был выполнен для трех срезов кристаллов кремния: (100), (110), (111). Полученные в работе результаты, могут быть использованы для оптимизации процесса лазерного разделения двухслойных структур из монокристаллического кремния и стекла.

**Ключевые слова:** лазерное раскалывание, кремниевая пластина, метод конечных элементов.

**Introduction.** The main methods of separating glass products and instrument wafers into crystals include: cutting with diamond disks, mechanical and laser scribing [1]–[3]. One of the effective ways to cut silicate glasses and monocrystalline silicon is laser splitting [1]–[8]. In some cases, the successful implementation of laser splitting technologies for silicon wafers and glass products can be achieved using double-beam processing methods [9]–[12]. The use of two-beam technologies is effective in processing structures consisting of various materials. Bilayer structures made of monocrystalline silicon and glass have become widespread in the manufacture of semiconductor microelectromechanical devices, while electrostatic bonding is one of the leading technologies for producing such samples [2], [13]. Paper [2] provides a study of the laser splitting process of bilayer structures made of silicon and glass, taking into consideration the anisotropy of the elastic properties of monocrystalline silicon using a laser beam with a wavelength of 1,06  $\mu\text{m}$ , focused from the side of the glass layer. Paper [12] presents a numerical simulation of the laser splitting process of bilayer structures made of monocrystalline silicon and glass when the workpiece is exposed to laser beams with wavelengths equal to 1.06  $\mu\text{m}$  and 10.6  $\mu\text{m}$  and a refrigerant. The current paper demonstrates the results of the finite-element simulation of laser splitting of bilayer structures made of monocrystalline silicon and glass during laser heating by beams with wavelengths equal to 0,808  $\mu\text{m}$  and 10,6  $\mu\text{m}$  and under the action of a refrigerant. Using laser radiation parameters with the wavelength of 0,808  $\mu\text{m}$  for simulation is relevant since silicon absorbs radiation with this wavelength quite intensively. It is worth noting that the experimental studies of the separation processes of silicon wafers into crystals in [4] were carried out with the setup that included a laser generating radiation at this wavelength.

**Numerical modeling.** The finite-element simulation of the laser splitting process of bilayer structures made of monocrystalline silicon and glass was carried out within the framework of an uncoupled thermoelasticity problem in the quasi-static formulation using ANSYS.

The criterion of maximum tensile stresses was used to determine the direction of laser-induced crack development [14].

When modeling, it was assumed that the thermal conductivity coefficient, specific heat capacity and density of the LC5 glass and monocrystalline silicon are constant and equal to  $\lambda_1=1,13$  W/m K,  $C_1 = 795$  J/Kg  $\cdot$ °C,  $\rho_1=2270$  kg/m<sup>3</sup> for glass and  $\lambda_2=109$  W/m K,  $C_2=758$  J/Kg $\cdot$ °C,  $\rho_2=2330$  kg/m<sup>3</sup> for silicon. The temperature dependences of the linear thermal expansion coefficients of the LC5 glass and single-crystal silicon were taken into account. The calculations considered the data on the values of the reflection and absorption coefficients of monocrystalline silicon and optical

glass for laser radiation with wavelengths of 0,808  $\mu\text{m}$  and 10,6  $\mu\text{m}$ . The modulus of elasticity and Poisson's ratio for glass were assumed to be equal to  $E_1 = 68,5 \text{ GPa}$ ,  $\nu_1 = 0,184$ . In the simulation, the following elastic stiffness constants of crystalline silicon were used:  $C_{11} = 165,6 \cdot \text{GPa}$ ,  $C_{12} = 63,9 \cdot \text{GPa}$ ,  $C_{44} = 79,5 \cdot \text{GPa}$  [2], [13], [15]–[20].

The calculations were performed for the following parameters of laser beams: radiation spot radius  $R_1 = 1 \cdot 10^{-3}$  for a beam with a radiation wavelength  $\lambda_1 = 0,808 \mu\text{m}$  and radiation power  $P_0 = 200 \text{ W}$ ; radiation spot radius  $R_2 = 1 \cdot 10^{-3} \text{ m}$  for a beam with a radiation wavelength  $\lambda_2 = 10,6 \mu\text{m}$  and radiation power  $P_0 = 10 \text{ W}$ . The calculations were carried out for bilayer disks made of monocrystalline silicon and glass with a radius of  $R = 15,5 \text{ mm}$  (the silicon layer thickness is  $H_1 = 0,5 \text{ mm}$ ; the glass layer thickness is  $H_2 = 0,5 \text{ mm}$ ). The sample travel speed relative to the laser beams and the refrigerant was  $V = 10 \text{ mm/s}$ .

To perform a comparative analysis, the thermoelastic field distribution was calculated for six spatial variants of the laser radiation and refrigerant impact zones:

A) laser splitting of the bilayer structure with sequential laser heating by beams with wavelengths equal to 0,808  $\mu\text{m}$  and 10,6  $\mu\text{m}$  and under the action of the refrigerant from the side of monocrystalline silicon (see Figure 1, the horizontal arrow indicates the direction of movement of the product relative to the laser beams and the refrigerant);

B) laser splitting of the bilayer structure with sequential laser heating by a beam with a wavelength of 0,808  $\mu\text{m}$  and under the action of the refrigerant from the side of monocrystalline silicon (see Figure 2);

C) laser splitting of the bilayer structure during laser heating by a beam with a wavelength of 0,808  $\mu\text{m}$  from the side of monocrystalline silicon (see Figure 3);

D) laser splitting of the bilayer structure with sequential laser heating by beams with wavelengths equal to 0,808  $\mu\text{m}$  and 10,6  $\mu\text{m}$  and under the action of the refrigerant from the side of the glass layer;

E) laser splitting of the bilayer structure with sequential laser heating by a beam with a wavelength of 0,808  $\mu\text{m}$  and under the action of the refrigerant from the side of the glass layer;

F) laser splitting of the bilayer structure during laser heating by a beam with a wavelength of 0,808  $\mu\text{m}$  from the side of the glass layer.

The mutual location of the impact zones of the laser beams and the refrigerant for treatment variants D, E, F coincides with variants A, B, C, respectively, taking into account their impact from the glass layer. The mutual location of laser beams and refrigerant exposure areas for treatment variants D, E, F coincides with variants A, B, C, taking into account their exposure from the side of the glass layer.

Thermoelastic fields in the bilayer structure for each of the six spatial variants of the laser and refrigerant impact zones were calculated for six different variants, taking into account the anisotropy of the silicon layer, i.e. I a is the analysis of the (100) cut when cutting in the [001] direction; I b is the (100) cut analysis when cutting in the [011] direction; II a is the (110) cut analysis when cutting in the direction [110]; II b is the analysis of the (110) cut when cutting in the [001] direction; II c is the (110) cut analysis, when cutting in the [111] direction, III is the analysis of the (111) cut, when cutting in the [110] direction.

The results of the calculations are presented in Tables 1–2 and in Figures 4–8.

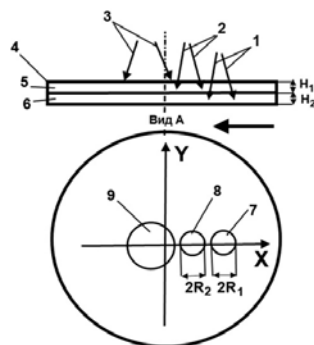


Figure 1 – Spatial arrangement of the impact zones of laser radiation and a refrigerant (variant A): 1 is the laser beam with a wavelength of 0,808  $\mu\text{m}$ , 2 is the laser beam with a wavelength of 10,6  $\mu\text{m}$ , 3 is the refrigerant, 4 is the processed bilayer structure made of monocrystalline silicon 5 and glass 6, 7 is the laser beam cross-section 1 on the working plane, 8 is the laser beam cross-section 2 on the working plane, 9 is the refrigerant impact zone

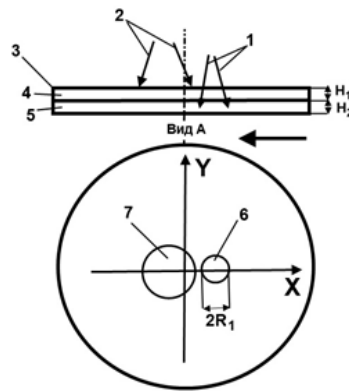


Figure 2 – Spatial arrangement of the impact zones of laser radiation and a refrigerant (variant B): 1 is the laser beam with a wavelength of  $0,808 \mu\text{m}$ , 2 is the refrigerant, 3 is the processed bilayer structure made of monocrystalline silicon 4 and glass 5, 6 is the laser beam cross-section 1 on the working plane, 7 is the refrigerant impact zone

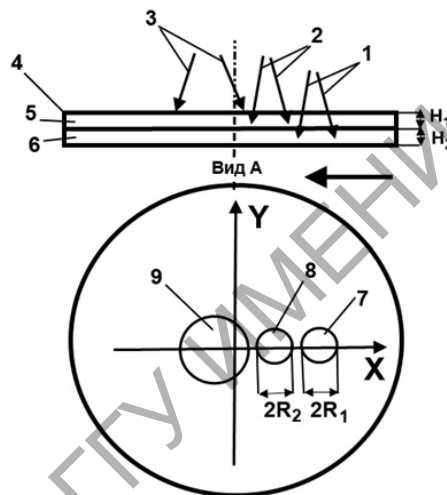


Figure 3 – Spatial arrangement of the impact zones of laser radiation and a refrigerant (variant C): 1 is the laser beam with a wavelength of  $0,808 \mu\text{m}$ , 2 is the processed bilayer structure made of monocrystalline silicon 3 and glass 4, 5 is the laser beam cross-section 1 on the working plane

Table 1 shows the calculated values of the maximum and minimum temperatures in the processed bilayer structure. Table 2 shows the calculated values of the maximum tensile and compressive stresses in the processing area.

Figures 4–5 show the distributions of temperature fields and fields of thermoelastic stresses created in the bilayer structure for each of the six spatial variants of the location of the laser radiation and refrigerant impact zones when cutting in the  $[001]$  direction of the  $(100)$  cut of monocrystalline silicon (variant Ia). Letters a), b), c) indicate variants A, B, C of the spatial location of the laser radiation and refrigerant impact zones in Figures 4–5.

Due to the absence of thermal conductivity anisotropy in silicon crystals, the calculated temperatures in the laser processing zone for the  $(110)$ ,  $(100)$ , and  $(111)$  cuts coincide when choosing the same processing parameters.

The data (Table 1) show that the maximum temperature values for all six simulation modes do not exceed the glass softening temperature. Thus, the calculated values of temperatures are in the range necessary for implementing brittle fracture of a bilayer wafer under the action of thermo-elastic stresses.

In general, the peculiarities of the temperature fields localization, presented in Figures 4 and 6, coincide with the results of modeling the process of laser splitting of bilayer structures made of silicon and glass using laser radiation with a wavelength of  $1,06 \mu\text{m}$  [14]. More intense absorption of radiation with a wavelength of  $0,808 \mu\text{m}$  by silicon was taken into account.

Table 1 – Calculated values of the maximum and minimum temperatures in the processed bilayer structure

Temperature in the processed bilayer structure T, K	Variant of the location of the laser radiation and refrigerant impact zones					
	A	B	C	D	E	F
maximum	784	675	782	856	845	863
minimum	295	294	298	295	295	299

As mentioned earlier, Table 2 shows the calculated values of the maximum tensile and compressive stresses created in the processing area during laser splitting for six spatial variants of the location of the laser radiation and refrigerant impact zones and for six different variants that take into account the silicon layer anisotropy.

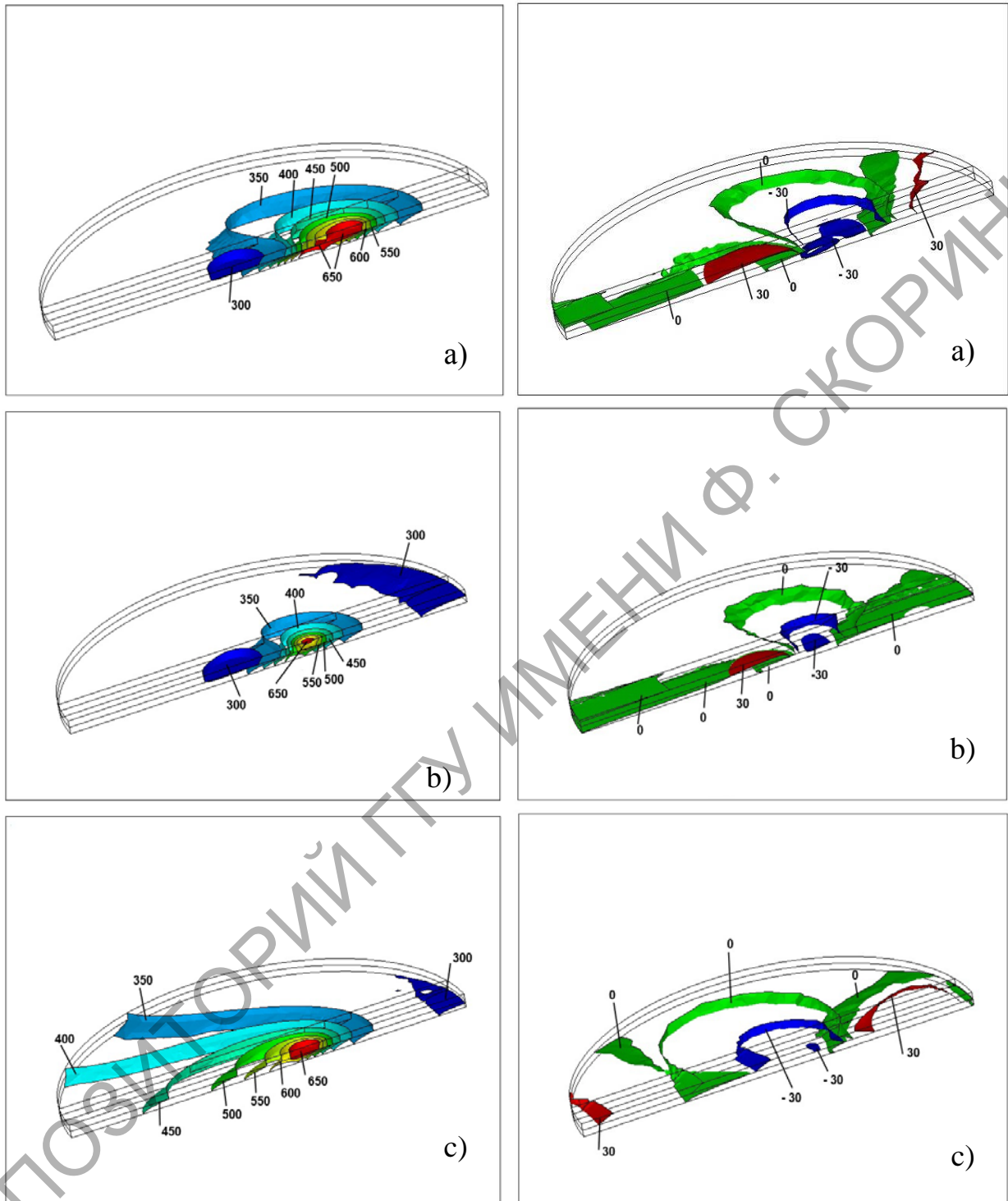
Table 2 – Calculated values of the maximum tensile and compressive stresses in the processing area of the bilayer structure

Silicon cut variant	Maximum stresses in the processing area $\sigma_{yy}$ , MPa	Variant of the location of the laser radiation and refrigerant impact zones					
		A	B	C	D	E	F
Ia	tensile	64	46	42	63	46	59
	compressive	185	148	172	231	239	230
Ib	tensile	68	49	45	60	45	63
	compressive	184	149	170	229	240	227
IIa	tensile	65	46	49	69	47	63
	compressive	199	158	185	249	256	285
IIb	tensile	76	56	49	72	56	63
	compressive	220	176	205	287	297	285
IIc	tensile	73	53	53	67	50	70
	compressive	209	168	194	265	277	265
III	tensile	81	59	48	65	49	67
	compressive	235	187	219	298	307	297

The data analysis (see Table 2) shows that the difference in the values of the maximum tensile stresses in bilayer structures caused by the silicon anisotropy reaches 28%. The difference in the values of the maximum tensile stresses, due to the spatial arrangement of the laser radiation and refrigerant impact zones, reaches 55%. In this case, the highest tensile stress values are achieved for the combination (III, A) when splitting the cut (111) when the laser beams and the refrigerant move in the direction [110] from the side of monocrystalline silicon. The smallest tensile stress values are achieved for the combination (Ia, C) when splitting the cut (100) when the laser beam with a wavelength of 1,06  $\mu\text{m}$  moves in the [001] direction from the side of monocrystalline silicon.

The calculated values of the corresponding tensile stresses in the processing area are 81 MPa and 42 MPa. Considering the above differences in the values of thermoelastic stresses, it seems appropriate to choose the technological parameters of the process of separating bilayer structures by the method of laser splitting (for example, by changing the processing speed or the power of laser radiation).

Let us pay attention to the features of the spatial localization of thermoelastic fields created as a result of laser splitting of bilayer structures when implementing various options for the spatial arrangement of the laser radiation and refrigerant impact zones. Figure 5 demonstrates that when implementing the variants with the refrigerant, significant tensile stresses are created in the zone of its influence on the surface of the processed sample (see Figures 5a, 5b). In the case of single-beam processing variants, areas of significant tensile stresses are also formed in the bilayer structure but at a significant distance from the center of the laser beam (see Figure 5c). In practice, this leads to instability of the laser splitting process and the possibility of deflection of laser-induced cracks from the processing line. The spatial configuration analysis of the boundary between tensile and compressive stresses in bilayer structures in the processing zone (see isosurfaces at  $\sigma_{yy} = 0$ ) allows predicting the success of crack propagation in both layers of the bilayer structure. In this case, the most effective is the use of laser splitting of the bilayer structure with sequential laser heating and under the action of the refrigerant from the side of monocrystalline silicon (see Figures 5a and 5b). Note that similar features were observed when simulating the laser splitting process of bilayer structures made of silicon and glass using laser radiation with a wavelength of 1,06  $\mu\text{m}$ .



a) double-beam exposure with the refrigerant;  
 b) laser impact with a wavelength of 0,808 μm and the refrigerant; c) laser impact with a wavelength of 0,808 μm

Figure 4 – Temperature distribution in the volume of the processed bilayer sample in processing from the side of monocrystalline silicon, K

a) double-beam exposure with the refrigerant;  
 b) laser impact with a wavelength of 0,808 μm and the refrigerant; c) laser impact with a wavelength of 0,808 μm

Figure 5 – Distribution of stresses  $\sigma_{yy}$  in the volume of the processed bilayer sample in processing from the side of monocrystalline silicon, MPa

**Conclusions.** The results obtained show the necessity to take into consideration the anisotropy of elastic properties of monocrystalline silicon when choosing the parameters of splitting bilayer structures made of silicon and glass when the workpiece is exposed to laser beams with wavelengths equal to 0,808  $\mu\text{m}$  and 10,6  $\mu\text{m}$  and a refrigerant. The paper shows the feasibility of implementing laser splitting of a bilayer structure with sequential laser heating and under the action of the refrigerant from the side of monocrystalline silicon.

### References

1. Nisar, S. Laser glass cutting techniques / S. Nisar, L. Li, M. Sheikh // A Review, Journal of Laser Applications. – 2013. – V. 25, № 4. – P. 042010.
2. Cai, Y. C. Laser cutting silicon-glass double layer wafer with laser induced thermal-crack propagation / Y. C. Cai, L. J. Yang, H. Z. Zhang, Y. Wang // Opt. Laser. Eng. – 2016. – V. 82. – P. 173–185.
3. Method of cutting plates from fragile materials : pat. № 2404931 / V. S. Kondratenko, A. S. Naumov. – Publ. 27.11.2010.
4. Naumov, A. S. Development of division technology of instrument wafers on crystals : author's abstract of Ph.D. of physics dissertation : 05.11.14 / A. S. Naumov ; MSUPI. – M., 2009. – 20 p.
5. The method of cutting of nonmetallic materials : pat. № 2024441 / V. S. Kondratenko. – Publ. 15.12.1994.
6. Serdyukov, A. N. Features of controlled laser thermal cleavage of crystalline silicon / A. N. Serdyukov, S. V. Shalupaev, Yu. V. Nikitjuk // Crystallography. – 2010. – V. 55 (6). – P. 933–937.
7. Method of crystalline silicon separation by thermoelastic strains : pat. № 2497643 / A. N. Serdyukov, S. V. Shalupaev, J. V. Nikitjuk, V. F. Sholokh. – Publ. 10.11.2013.
8. Saman, A. M. A study on separating of a silicon wafer with moving laser beam by using thermal stress cleaving technique / A. M. Saman, T. Furumoto, T. Ueda, A. Hosokawa // J. Mater. Process. Tech. – 2015. – V. 223. – P. 252–261.
9. Sysoev, V. K. Two laser thermo cleavage of glass elements for space-craft conception / V. K. Sysoev, P. A. Vyatlev, A. V. Chirkov [et al.] // Space journal of «Lavochkin association». – 2011. – V. 1. – P. 38–44.
10. Numerical study on thermal stress cutting of silicon wafer using two-point pulsed laser / J. Liu, J. Lu, X. Ni [et al.] // Optica Applicata. – 2011. – V. XLI, № 1. – P. 247–255
11. Junke, J. Cutting glass substrates with dual-laser beams / J. Junke, W. Xinbing // Optics and Lasers in Engineering. – 2009. – V. 47. – P. 860–864.
12. Nikitjuk, Y. V. Investigation of the process of laser splitting of two-layer structures of silicon plates and glass substrates / Y. V. Nikitjuk // Problems of Physics, Mathematics and Technics. – 2020. – V. 44, № 3. – P. 44–49.
13. Sinev, L. S. Calculation and selection of silicon to glass anodic bonding modes based on the criterion of minimum residual stress : diss. ... cand. of engineering sciences : 05.27.06 / L. S. Sinev ; Bauman Moscow State Technical University. – M., 2016. – 119 p.
14. Karzov, G. P. Physico-mechanical modeling of destruction processes / G. P. Karzov, B. Z. Margolin, V. A. Shevtsova. – SPb. : Polytechnic, 1993. – 391 p.
15. Reference book on electrical materials / Yu. V. Koritsky [et al.]. – L. : Energoatomizdat, 1988. – 728 p.
16. Lackner, T. Determination of axisymmetric elastic constants in anisotropic silicon for a thyristor tablet / T. Lackner // Journal of electronic materials. – 1989. – V. 18. – P. 19–24.
17. Acoustic crystals / A. A. Blistanov [et al.] ; under total. ed. M. P. Shaskolskaya. – M. : Nauka, 1982. – 632 p.
18. Technology of semiconductor silicon / E. S. Falkevich [et al.]. – M. : Metallurgy, 1992. – 408 p.
19. Kontsevov, Yu. A. Plasticity and strength of semiconductor materials and structures / Yu. A. Kontsevov, Yu. M. Litvinov, E. A. Fattakhov. – M. : Radio and communication, 1982. – 240 p.
20. Colorless optical glass. Physicochemical properties. Parameters : GOST 13659-68. – Put in. 01.01.1969. M., 1968. – 60 p.

<sup>1</sup>Гомельский государственный университет имени Франциска Скорины

<sup>2</sup>Университет гражданской защиты МЧС Республики Беларусь